JACS
JOURNAL OF THE AMERICAN CHEMICAL SOCIETY
Communication
pubs.acs.org/JACS

Spectral Tuning of Rhodopsin and Visual Cone Pigments

Xiuwen Zhou,[†] Dage Sundholm,[‡] Tomasz A. Wesołowski,[†] and Ville R. I. Kaila*[,§]

[†]Département de Chimie Physique, Université de Genève, 30 quai Ernest-Ansermett, CH-1211 Genève 4, Switzerland
[‡]Department of Chemistry, P.O. Box 55, A. I. Virtanens plats 1, University of Helsinki, FIN-00014 Helsinki, Finland
[§]Department Chemie, Technische Universität München, Lichtenbergstrasse 4, D-85747 Garching, Germany

Supporting Information

ABSTRACT: Retinal is the light-absorbing biochromophore responsible for the activation of vision pigments and light-driven ion pumps. Nature has evolved molecular tuning mechanisms that significantly shift the optical properties of the retinal pigments to enable their absorption of visible light. Using large-scale quantum chemical calculations at the density functional theory level combined with frozen density embedding theory, we show here how the protein environment of vision pigments tunes the absorption of retinal by electrostatically dominated interactions between the chromophore and the surrounding protein residues. The calculations accurately reproduce the experimental absorption maxima of rhodopsin and the red, green, and blue color pigments. We further identify key interactions responsible for the color-shifting effects by mutating the rhodopsin structure *in silico*, and we find that deprotonation of the retinyl is likely to be responsible for the blue-shifted absorption in the blue cone vision pigment.

Retinal is a conjugated polyene that occurs in the light-capturing unit of several photobiological systems. In vision pigments[1] and bacterial light-driven proton pumps,[2] retinal is covalently linked to the protein by a lysine residue, forming a Schiff base (SB). The protein environment shifts the absorption maximum of retinal from 365−430 nm (2.80−3.40 eV) in aqueous solution to 420−560 nm (2.20−2.95 eV) in the vision proteins,[1] enabling their absorption of visible light. The exact molecular mechanism of the spectral shift has remained elusive for more than half a century. It has been suggested that the tuning may arise from an altered conjugation of the polyene,[3] by specific electrostatic interactions between protein residues and the retinal,[4] and by charge transfer and polarization effects.[5] The development of accurate electronic structure theory methods open up new ways of addressing the molecular mechanism of spectral tuning.

In this study, we investigate the protein-induced spectral shifts of retinal in rhodopsin and its homologous color cone pigments using large-scale quantum chemical calculations. Rhodopsin is a protein in the rod cells of the vertebrate eye, responsible for dim vision.[1] Color vision takes place in the cone cells and is catalyzed by three color pigment proteins, responsible for the absorption of red, green, and blue photons, respectively.[1b] Light absorption by these G-protein coupled receptors leads to an 11-*cis* to all-*trans* isomerization of the retinyl side chain, activating a G-protein-mediated signaling cascade that triggers the vision process.[1]

Photobiological systems face unique computational challenges due to their complex chromophore−protein environment, which must be explicitly considered using large computational models.[6] Although *ab initio* methodologies can accurately predict optical transitions in molecules, most such methods are inapplicable to photobiology due to their high computational costs. Recent developments, such as the restricted virtual space approach in combination with low-order correlation methods, increase the possibility of treating large photobiological systems.[4c,7] However, due to the high computational scaling of such methods, extensive studies of the chromophore−protein interactions beyond the immediate chromophore vicinity are demanding.

We use here a frozen-density embedding theory (FDET)[8] based method to compute the vertical excitation energies of retinal embedded in large protein surroundings, within the linear-response time-dependent density functional theory (TDDFT)[9] framework. In these calculations, we treat the chromophore region as an active system that is quantum chemically embedded in a frozen electron density of surrounding protein residues. Due to the large computational savings introduced by treating the surroundings as a frozen electron density, the FDET approach allows the modeling of the chromophore−protein interactions at full quantum mechanical level, using system sizes comprising ∼400 atoms, usually beyond the capabilities of conventional TDDFT methods, especially when a large number of calculations are necessary, as in this work.

Molecular models of rhodopsin and of the red, green, and blue cone pigments were constructed on the basis of coordinates of the crystal structure from *Bos taurus*[11] and the homology models obtained from Brookhaven Protein Data Bank (PDB IDs: 1U19, 1KPX, 1KPN, 1KPW).[12] The models comprised 329−370 atoms, with the retinal surrounded by 25−30 residues nearest to the chromophore binding pocket (see SI Table 1, SI Figures 1 and 2). All amino acid residues were cut at the C_β atoms, which were saturated by hydrogen atoms. The models were structure optimized using the BP86 functional with the RI-MARIJ approximation and def2-SVP basis sets.[13] The retinal side chain and hydrogen atoms in the surrounding residues were allowed to fully relax in the structure optimization. To study the saturation of these models, the CHARMM27 force field[14] was used to embed the quantum chemical models in the point charge surroundings of the protein residues beyond the QM model

Received: November 21, 2013
Published: January 14, 2014

   dx.doi.org/10.1021/ja411864m | J. Am. Chem. Soc. 2014, 136, 2723−2726

systems. Based on structural alignment, sequence comparison (SI Figure 1, SI Table 1), and the X-ray structure of rhodopsin,[11] we also constructed blue (Rh:Δblue) and red mutant (Rh:Δred) models to probe the function of key residues responsible for the tuning process.[1b] The Rh:Δblue model comprised the *in silico* mutations W265Y, Y191W, E122L, H211C, G90C, A124T, A292S, A295S, and A299C, whereas the Rh:Δred model comprised E181H, E122L, F208M, H211C, F212C, and optimized similar to the rhodopsin and cone pigment models (Cartesian coordinates are given in the SI). To study alternative protonation states of the retinal, we performed local optimizations of the SB proton with the proton constrained to reside either on Glu-113 or on the retinyl side chain. The optimizations were performed using a hybrid quantum/classical mechanics (QM/MM) approach at the B3LYP/def2-SVP/CHARMM27 level of theory.[14,15] Only the Glu-113/SB retinal was modeled for the QM system, and the remaining system was treated classically. After the QM/MM optimization, the structure of the Glu-113/SB pair was incorporated back into the large full-QM models. For computation of vertical excitation energies, the optimized structures were separated into an embedded active system and an environment region. The embedded active system comprised (i) the retinyl chromophore or (ii) the retinal and Glu-113, which were studied using the B3LYP functional[15] and Slater-type orbitals (STO) of double-zeta quality augmented with polarization functions (DZP).[16] The frozen density of the environment is generated by a Kohn−Sham calculation for the isolated environment at the BP86/DZP level. The electron density of the embedded subsystem, ρ_A, and the charge density of the embedding protein subsystem, ρ_B and ρ_B^{pos}, indicating electrons and nuclei, respectively, uniquely determine the embedding potential (v_{emb}), within the FDET framework:[8]

$$v_{emb}[\rho_A, \rho_B; r] = \int \frac{\rho_B^{pos}(\mathbf{r}')}{|\mathbf{r}' - \mathbf{r}|}d\mathbf{r}' + \int \frac{\rho_B(\mathbf{r}')}{|\mathbf{r}' - \mathbf{r}|}d\mathbf{r}' + \frac{\delta E_{xc}^{nad}[\rho_A, \rho_B]}{\delta \rho_A(\mathbf{r})} + \frac{\delta T_s^{nad}[\rho_A, \rho_B]}{\delta \rho_A(\mathbf{r})}$$

The nonadditive exchange-correlation component of the embedding potential was approximated using the local-density approximation for $E_{xc}[\rho]$,[17] whereas the nonadditive kinetic component was approximated using the NDSD bifunctional.[18] This leads to a robust computational protocol that reduces possible errors due to the approximations in the nonadditive kinetic energy.[19] For FDET/TDDFT calculations beyond the Neglect of Dynamic Response of the Environment approximation, the reader should consult the recent comprehensive review by Neugebauer.[20] Since the charge-transfer excitations are more sensitive to the choice of frozen density in FDET calculations than local excitations, additional calculations were performed using the CAM-B3LYP[21] functional as implemented in ADF.[22] We did not observe noticeable TDDFT charge-transfer problems for any of studied systems with retinal comprising the embedded active region (see also SI Table 2). Moreover, test calculations on a *cis*-retinal model at the coupled-cluster approximate singles and doubles (CC2) level[23] (SI Table 3) suggest that the long-range corrected density functional CAM-B3LYP consistently overestimates the excitation energies by ∼0.3 eV in comparison to the CC2 and experimental data (SI Tables 2−4). We thus treated the chromophore at the B3LYP level in all reported calculations. The electronic excitation energies of the embedded retinal subsystem were obtained using

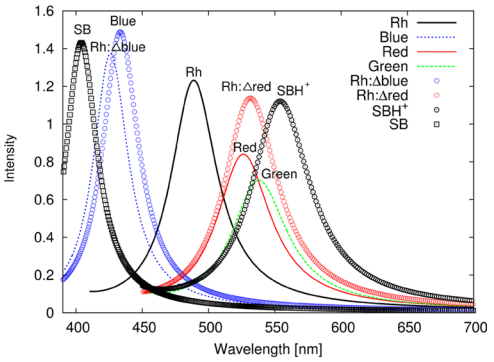

Figure 1. Computed absorption spectra of retinal models in vacuum (SBH^+/SB), and embedded in the protein surroundings of rhodopsin (Rh), the red, green, and blue photopigments (red/green/blue), and *in silico* constructed red and blue mutant pigments of rhodopsin (Rh:Δred/Δblue). The vertical excitation energies and oscillator strengths were obtained using FDET/TDDFT calculation at the B3LYP/DZP level. The intensities are Lorentz broadened with a width that is 0.5% of the frequency range and based on computed oscillator strengths.

the FDET/TDDFT method implemented[24] in ADF[22] versions 2012.01 and 2013.01. The structure optimizations were performed using TURBOMOLE[25] version 6.3 and CHARMM/Q-Chem version 4.0.[26]

The computed absorption spectra for the isolated and protein embedded retinal models are shown in Figure 1. We obtain an excitation energy of 2.54 eV (488 nm) for retinal embedded in rhodopsin, which agrees well with the experimental absorption maximum of 2.49 eV (498 nm).[29] For the red and green pigments, we obtain excitation energies of 2.36 eV (525 nm) and 2.30 eV (540 nm), respectively, whereas the blue pigment absorbs at 2.91 eV (426 nm), which is obtained by deprotonation of the SB, consistent with our previous study.[4c] We also explored different embedding strategies; the results are shown in SI Table 2. We find that the red pigment model has the largest apparent error of ∼0.16 eV in the excitation energy, within the expected error limit of TDDFT/B3LYP calculations.[7c] However, it is likely that uncertainties in the excitation energies may originate from the use of homology models for the cone pigments, for which there are uncertainties in the exact position of residues. Our excitation energies for rhodopsin obtained at the FDET/CAM-B3LYP level of theory are similar to values obtained in a recent detailed QM/MM study (see SI Table 2).[30]

The FDET calculations suggest that the protein surroundings of rhodopsin and the cone pigments absorbing red and green light *electrostatically* blue-shift the retinyl absorption by 0.3−0.45 eV (Table 1) relative to the absorption maximum of retinal in vacuum (2.27 eV/546 nm). The protein induced excitation-energy shift (ΔE_{tot}) is obtained as the difference between the energies calculated for the completely relaxed chromophore in vacuum and in the protein. The electrostatic shift (E_{elec}) is determined by removing the frozen electron density of the surrounding protein residues and keeping the chromophore structure unchanged. This also removes the small Pauli repulsion, which must be included in the FDET embedding potential to obtain meaningful interaction energies.[24] The *steric tuning contribution* (E_{steric}) is obtained by subtracting the electrostatic contribution from the total protein shift. The steric contribution red-shifts the absorption energies by 0.07−0.27 eV in all models, due to a destabilization of the ground state relative to the excited state. This suggest that electrostatic effects

dx.doi.org/10.1021/ja411864m | *J. Am. Chem. Soc.* 2014, 136, 2723−2726

Table 1. Calculated (E_{FDET}) and Experimental (E_{exp})[3,34] Vertical Excitation Energies (VEE, in eV) and Protein-Induced Shift (ΔE) of Models of Rhodopsin, the Red, Green, and Blue Cone Pigments, and the Blue- (Rh:Δblue) and Red-Shifted (Rh:Δred) *in Silico* Mutant Models of Rhodopsin[a]

system	state	E_{FDET}	E_{isol}	E_{exp}	ΔE_{tot} [E_{elec}/E_{steric}]
Rh	SBH^+/E^-	2.54 (488)	2.09 (593)	2.49 (498)	+0.27 [+0.45/−0.18]
red	SBH^+/E^-	2.36 (525)	2.04 (608)	2.21 (560)	+0.09 [+0.32/−0.23]
green	SBH^+/E^-	2.30 (539)	2.00 (620)	2.32 (534)	+0.03 [+0.30/−0.27]
blue	SB/EH	2.91 (426)	2.90 (428)	2.92 (425)	−0.14 [+0.01/−0.15]
Rh:Δred	SBH^+/E^-	2.33 (532)	2.20 (564)	–	+0.06 [+0.13/−0.07]
Rh:Δblue	SB/EH	2.86 (434)	2.86 (434)	–	−0.19 [+0.00/−0.19]
retinal	SBH^+	–	2.27 (546)	2.03 (610)	–
retinal	SB	–	3.05 (407)	–	–

[a]The calculated values are obtained at the FDET/TDDFT (B3LYP/DZP) level for protein models, with retinal in the embedded active system. E_{isol} is the VEE of the protein-environment-free chromophore, at TDDFT level. SH^+ and S refer to the protonated and deprotonated Schiff base retinal, and E^-/EH to the protonation state of Glu-113.

dominate the spectral tuning of the protonated SB retinal, consistent with earlier results by Coto et al.[31] and Hasegawa et al.[32] However, our calculations indicate that the steric contribution becomes dominating for the blue-cone model, which is electrostatically tuned by only 0.01 eV due to deprotonation of the SB retinal.

The electrostatic tuning mechanism originates from the photophysical properties of the retinal chromophore. The frontier orbitals involved in the excitation, shown in Figure 2, suggest that the retinal excitation has a $\pi\rightarrow\pi^*$ character and results in a redistribution of the charge with the positive charge of the SB transferred toward the β-ionine ring (SI Table 5), a well-known property for retinal.[4,33] This charge transfer makes the retinyl susceptible for electrostatic stabilization by charges and dipoles in the surrounding protein residues. Positive charges or dipoles near the SB, or negative charges near the β-ionine group are found to cause a red shift by stabilizing the excited state with respect to the ground state. In contrast, negative charges and dipoles near the SB, or positive charges near the β-ionine group lead to a blue shift by stabilizing the ground state. Consistent with these findings, we observe that in the *in silico* mutated Rh:Δred model, an increased number of cystein and methionine residues near the β-ionine ring has a red-shifting effect of 0.21 eV, shifting the absorption maximum from 488 to 532 nm. Consistently, we find in the *in silico* mutated Rh:Δblue model that replacing nonpolar residues (G90, A292, A295) near the SB with polar serine and threonine residues has a blue-shifting effect of 0.32 eV, shifting the absorption maximum from 488 to 434 nm.

The blue-shifting effect is strengthened by removing polar residues near the β-ionine and decreasing the aromatic stacking of the retinyl by the W265Y substitution, which may lead to a decreased π-cation interaction in the excited state. However, the interpretation of the tuning effects in Rh:Δblue is more complex as compared to the Rh:Δred model. Similarly to the blue cone pigment, the retinyl SB in the Rh:Δblue becomes deprotonated in the geometry optimization, which most likely has the largest

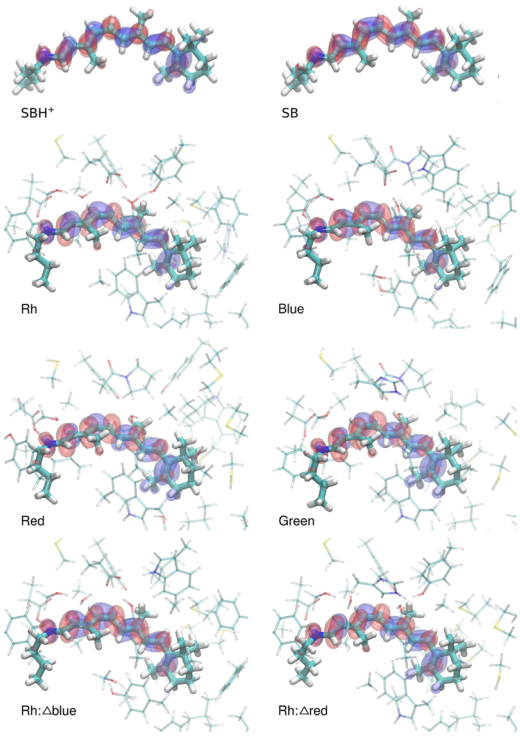

Figure 2. Frontier orbitals involved in the $\pi\rightarrow\pi^*$ photoexcitations of retinal models in vacuum (SBH^+/SB), and embedded in the protein surroundings of rhodopsin (Rh), the red, green, and blue photopigments (red/green/blue), and *in silico* constructed red and blue mutant pigments of rhodopsin (Rh:Δred/Δblue). The figure was prepared using VMD.[27]

blue-shifting effect. The excitation in the deprotonated SB retinal leads to a significantly smaller charge separation than that for the protonated retinal (SI Table 5). Thus, the deprotonated retinal is less sensitive to electrostatic tuning effects, consistently with the larger steric tuning contribution shown in Table 1. The red and blue shifts achieved by substituting the adjacent amino acids are consistent with the spectral shifts observed in previous site-directed mutagenesis experiments.[1b,28] Moreover, the observed spectral shifts and tuning effects of the red-pigment model are also consistent with the retinal−charge/dipole model calculations of the protonated SB retinal shown in SI Figure 2.

To better understand the balance between red- and blue-shifting effects in the tuning process, we performed additional FDET calculations on protein models with Glu-113 removed. In agreement with the pioneering study of rhodopsin tuning by Coto et al.,[31] we find that Glu-113 imposes a blue-shifting effect, while the remaining protein environment causes a red shift (SI Table 6). Our FDET calculations suggest that the blue-shifting effect of Glu-113 varies between 0.2 and 0.4 eV (SI Table 6), thus indicating that the remaining protein environment tunes the blue-shifting effect of this residue. We analyzed the electrostatic potential (ESP) charges of Glu-113 in the different models, and found a variation of up to 0.2*e* (SI Figure 3), suggesting that the remaining protein environment indeed imposes a secondary polarization effect, which may in turn modulate the blue-shifting effect of Glu-113. Different electrostatic polarization of the retinyl side chain was previously described for the pigment models by Hasegawa et al.,[32] who suggested that the polarization of the ESP along the retinyl backbone causes a shift in the LUMO energy, thus changing the excitation energy. They found a somewhat higher blue-shifting effect of 0.7 eV for Glu-113, but

dx.doi.org/10.1021/ja411864m | J. Am. Chem. Soc. 2014, 136, 2723−2726

only a small variation in this effect among the different cone pigments, which may relate to the smaller QM region used in their calculations.

In summary, we discuss here a molecular basis for understanding the mechanism of the spectral tuning in vision pigments. Using large-scale quantum chemical FDET calculations and the TDDFT formalism, our computed vertical excitation energies are in quantitative agreement with experimental absorption maxima. We find that the protein-induced shifts are dominated by electrostatic interactions for the models with a protonated SB retinal, and that for them the observed tuning effects can be explained in terms of an electrostatic interaction model. We find that negative charges and dipoles near the β-ionine ring stabilizes the excited state causing a red-shifting effect, and that negative protein charges and dipoles near the SB stabilize the ground state relatively to the excited state leading to a blue shift on the absorption spectrum. We also find that the strongly blue-shifting effect of Glu-113 is modulated by the remaining protein environment in the different visual pigments. Moreover, the calculations predict that a deprotonated chromophore is responsible for the photon absorption of the blue-cone pigment. The presented large-scale quantum chemical calculations may form a basis for a rational photobiological design of proteins with specifically tuned absorption properties.[35]

■ ASSOCIATED CONTENT

Supporting Information

SI Tables 1−5, SI Figures 1−3, and coordinates of studied systems. This material is available free of charge via the Internet at http://pubs.acs.org.

■ AUTHOR INFORMATION

Corresponding Author

ville.kaila@ch.tum.de

Notes

The authors declare no competing financial interest.

■ ACKNOWLEDGMENTS

The Biowulf cluster at NIH and CSC—the Finnish IT Center for Science—are acknowledged for computer time. This research was supported by the Academy of Finland through projects (137460 and 266227) and its Computational Science Research Programme (258258). Grants from Swiss National Science Foundation (200020/134791/1 FNRS), COST Action CM1002, and Magnus Ehrnrooth Foundation are greatly appreciated.

■ REFERENCES

(1) (a) Palczewski, K. *Annu. Rev. Biochem.* **2006**, *75*, 743. (b) Kochendoerfera, G. G.; Lin, S. W.; Sakmar, T. P.; Mathies, R. A. *Trends Biochem. Sci.* **1999**, *24*, 300.

(2) Lanyi, J. K. *Annu. Rev. Physiol.* **2004**, *66*, 665.

(3) Blatz, P. E.; Liebman, P. *Exp. Eye Res.* **1973**, *17*, 573.

(4) (a) Wanko, M.; et al. *J. Phys. Chem. B* **2005**, *109*, 3606. (b) Andruniow, T.; Ferre, N.; Olivucci, M. *Proc. Natl. Acad. Sci. U.S.A.* **2004**, *101*, 17908. (c) Kaila, V. R. I.; Send, R.; Sundholm, D. *J. Phys. Chem. B* **2012**, *116*, 2249.

(5) Baasov, T.; Friedman, N.; Sheves, M. *Biochemistry* **1987**, *26*, 3210.

(6) Neugebauer, J. *Chem. Phys. Chem.* **2009**, *10*, 3148.

(7) (a) Send, R.; Kaila, V. R. I.; Sundholm, D. *J. Chem. Phys.* **2011**, *134*, 214114. (b) Kaila, V. R. I.; Send, R.; Sundholm, D. *Phys. Chem. Chem. Phys.* **2013**, 4491. (c) Send, R.; Kaila, V. R. I.; Sundholm, D. *J. Chem. Theory Comput.* **2011**, *799*, 2473.

(8) (a) Wesolowski, T. A.; Warshel, A. *J. Phys. Chem.* **1993**, *97*, 8050. (b) Wesolowski, T. A. *Computational Chemistry: Reviews of Current Trends*, Vol. *X*; World Scientific, 2006. (c) Wesolowski, T. A. *Phys. Rev. A* **2008**, *77*, 012504. (d) Pernal, K.; Wesolowski, T. A. *Int. J. Quantum Chem.* **2009**, *109*, 2520.

(9) (a) Casida, M. E. In *Recent Advances in Density-Functional Methods, Part I: Time-dependent density-functional response theory for molecules*; Chong, D. P., Ed.; World Scientific: Singapore, 1995. (b) Casida, M. E. *J. Mol. Struct.: THEOCHEM* **2009**, *914*, 3. (c) Casida, M. E.; Wesolowski, T. A. *Int. J. Quantum Chem.* **2004**, *96*, 577.

(10) Dreuw, A.; Head-Gordon, M. *Chem. Rev.* **2005**, *105*, 4009.

(11) Okada, T.; Sugihara, M.; Bondar, A. N.; Elstner, M.; Entel, P.; Buss, V. *J. Mol. Biol.* **2004**, *342*, 571.

(12) Stenkamp, R. E.; Filipek, S.; Driessen, C. A.; Teller, D. C.; Palczewski, K. *Biochim. Biophys. Acta* **2002**, *1565*, 168.

(13) (a) Becke, A. D. *Phys. Rev. A* **1988**, *38*, 3098. (b) Perdew, J. P. *Phys. Rev. B* **1986**, *33*, 8822. (c) Sierka, M.; Hogekamp, A.; Ahlrichs, R. *J. Chem. Phys.* **2003**, *118*, 9136. (d) Weigend, F.; Ahlrichs, R. *Phys. Chem. Chem. Phys.* **2005**, *7*, 3297.

(14) MacKerell, A. D., Jr.; et al. *J. Phys. Chem. B* **1998**, *102*, 3586.

(15) (a) Becke, A. D. *J. Chem. Phys.* **1993**, *98*, 5648. (b) Lee, C. T.; Yang, W. T.; Parr, R. G. *Phys. Rev. B* **1988**, *37*, 785.

(16) van Lenthe, E.; Baerends, E. J. *J. Comput. Chem.* **2003**, *24*, 1142.

(17) (a) Hohenberg, P.; Kohn, W. *Phys. Rev.* **1964**, *136*, B864. (b) Kohn, W.; Sham, L. J. *Phys. Rev.* **1965**, *140*, A1133.

(18) Garcia Lastra, J. M.; Kaminski, J. W.; Wesolowski, T. A. *J. Chem. Phys.* **2008**, *129*, 074107.

(19) Humbert-Droz, M.; Zhou, X.; Shedge, S. V.; Wesolowski, T. A. *Theor. Chem. Acc.* **2013**, *132*, 1405.

(20) Neugebauer, J. *Phys. Rep.* **2010**, *489*, 1.

(21) Yanai, T.; Tew, D. P.; Handy, N. C. *Chem. Phys. Lett.* **2004**, *393*, 51.

(22) ADF, SCM: Theoretical Chemistry, Vrije Universiteit, Amsterdam, The Netherlands, http://www.scm.com.

(23) Christiansen, O.; Koch, H.; Jørgensen, P. *Chem. Phys. Lett.* **1995**, *243*, 409.

(24) (a) Wesolowski, T. A. *J. Am. Chem. Soc.* **2004**, *126*, 11444. (b) Dulak, M.; Wesolowski, T. A. *Int. J. Quantum Chem.* **2005**, *101*, 543. (c) Jacob, C. R.; Neugebauer, J.; Visscher, L. *J. Comput. Chem.* **2008**, *29*, 1011.

(25) Ahlrichs, R.; Bär, M.; Häser, M.; Horn, H.; Kölmel, C. *Chem. Phys. Lett.* **1989**, *162*, 165. (http://www.turbomole.com)

(26) (a) Brooks, B. R.; et al. *J. Comput. Chem.* **2009**, *30*, 1545. (b) Shao, Y. *Phys. Chem. Chem. Phys.* **2006**, *8*, 3172. (c) Woodcock, H. L., III; et al. *J. Comput. Chem.* **2007**, *28*, 1485.

(27) Humphrey, W.; Dalke, A.; Schulten, K. *J. Mol. Graphics* **1996**, *14*, 33.

(28) Lin, S. W.; Kochendoerfer, G. G.; Carroll, K. S.; Wang, D.; Mathies, R. A.; Sakmar, T. P. *J. Biol. Chem.* **1998**, *273*, 24583.

(29) Wald, G.; Brown, P. K. *J. Gen. Physiol.* **1953**, *37*, 189.

(30) Valsson, O.; Campomanes, P.; Tavernelli, I.; Rothlisberger, U.; Filippi, C. *J. Chem. Theory Comput.* **2013**, *9*, 2441.

(31) Coto, P. B.; Strambi, A.; Ferré, N.; Olivucci, M. *Proc. Natl. Acad. Sci. U.S.A.* **2006**, *103*, 1714.

(32) Fujimoto, K.; Hasegawa, J.; Nakatsuji, H. *Chem. Phys. Lett.* **2008**, *462*, 318.

(33) (a) Bonacic-Koutecky, V.; Köhler, K.; Michl, J. *Chem. Phys. Lett.* **1984**, *104*, 440. (b) Birge, R. R.; Murray, L. P.; Pierce, M. M.; Akita, H.; Balogh-Nair, V.; Findsen, L. A.; Nakanishi, K. *Proc. Natl. Acad. Sci. U.S.A.* **1985**, *82*, 4117.

(34) (a) Nathans, J. *Sci. Am.* **1989**, *260*, 42. (b) Oprian, D. D.; Asenjo, A. B.; Lee, N.; Pelletier, S. L. *Biochemistry* **1991**, *30*, 11367. (c) Merbs, S. L.; Nathans, J. *Nature* **1992**, *356*, 433. (d) Nielsen, I. B.; Lammich, L.; Andersen, L. H. *Phys. Rev. Lett.* **2006**, *743*, 018304.

(35) Wang, W.; et al. *Science* **2012**, *338*, 1340.